Miner Deposita (2015) 50:607–617
DOI 10.1007/s00126-014-0560-1

ARTICLE

Did the massive magnetite "lava flows" of El Laco (Chile) form by magmatic or hydrothermal processes? New constraints from magnetite composition by LA-ICP-MS

Sarah A. S. Dare · Sarah-Jane Barnes · Georges Beaudoin

Received: 24 June 2014 / Accepted: 1 October 2014 / Published online: 29 October 2014

Abstract The El Laco magnetite deposits consist of more than 98 % magnetite but show field textures remarkably similar to mafic lava flows. Therefore, it has long been suggested that they represent a rare example of an effusive Fe oxide liquid. Field and petrographic evidence, however, suggest that the magnetite deposits represent replacement of andesite flows and that the textures are pseudomorphs. We determined the trace element content of magnetite by laser ablation inductively coupled plasma mass spectrometry (LA-ICP-MS) from various settings at El Laco and compared them with magnetite from both igneous and hydrothermal environments. This new technique allows us to place constraints on the conditions under which magnetite in these supposed magnetite "lava flows" formed. The trace element content of magnetite from the massive magnetite samples is different to any known magmatic magnetite, including primary magnetite phenocrysts from the unaltered andesite host rocks at El Laco. Instead, the El Laco magnetite is most similar in composition to hydrothermal magnetite from high-temperature environments (>500 °C), such as iron oxide-copper-gold (IOCG) and porphyry-Cu deposits. The magnetite trace elements from massive magnetite are characterised by (1) depletion in elements considered relatively immobile in hydrothermal fluids (e.g. Ti, Al, Cr, Zr, Hf and Sc); (2) enrichment in elements that are highly incompatible with magmatic magnetite (rare earth elements (REE), Si, Ca, Na and P) and normally present in very low abundance in magmatic magnetite; (3) high Ni/Cr ratios which are typical of magnetite from hydrothermal environments; and (4) oscillatory zoning of Si, Ca, Mg, REE and most high field strength elements, and zoning truncations indicating dissolution, similar to that formed in hydrothermal Fe skarn deposits. In addition, secondary magnetite in altered, brecciated host rock, forming disseminations and veins, has the same composition as magnetite from the massive lenses. Euhedral magnetite lining both open-spaced veins in the brecciated host rock and along the walls of large, hollow chimneys in the massive magnetite lenses also displays oscillatory zoning and most likely formed by fluctuating composition and/or physio-chemical conditions of the fluid. Thus, the chemical fingerprint of magnetite from the supposed El Laco magnetite lava flows supports the hydrothermal model of metasomatic replacement of andesite lava flows, by dissolution and precipitation of magnetite from high-temperature fluids, rather than a magmatic origin from an effusive Fe oxide liquid.

Keywords Magnetite · Trace elements · Oscillatory zonation · Hydrothermal replacement · Fe oxide liquid

Editorial handling: B. Lehmann

Electronic supplementary material The online version of this article (doi:10.1007/s00126-014-0560-1) contains supplementary material, which is available to authorized users.

S. A. S. Dare (✉) · S.-J. Barnes
Département Sciences Appliquées, Université du Québec à Chicoutimi, Saguenay, QC G7H 2B1, Canada
e-mail: sdare@uOttawa.ca

G. Beaudoin
Département Géologie, Université Laval, Québec, QC G1V 0A6, Canada

Present Address:
S. A. S. Dare
Department of Earth Sciences, University of Ottawa, Ottawa, ON K1H 6N5, Canada

Introduction

The 2 Ma stratovolcano of El Laco, Northern Chile, is worldly renowned for its enigmatic magnetite "lava flows", which form a number of mainly stratabound iron oxide-apatite (IOA) deposits (500 Mt at 60 wt% Fe; Nyström and Henríquez 1994) on surface and immediately below (<300 m depth). The origin of

El Laco magnetite deposits and many other IOA deposits, such as Kiruna in Sweden (e.g. Nyström and Henríquez 1994; Jonsson et al. 2013), remains controversial. Proponents of a magmatic origin, based on field evidence that the massive magnetite ore at El Laco takes the form of lava flows and pyroclastic deposits, argue their formation from a volatile-rich, Fe oxide liquid that erupted from the volcano at high temperatures (Park 1961; Nyström and Henríquez 1994; Naslund et al. 2002; Tornos et al. 2011). In contrast, others have argued that the massive magnetite lenses at El Laco formed by metasomatic replacement of the andesite lava flows based on magnetite veins and breccias and hydrothermal alteration assemblages surrounding the deposits (Hildebrand 1986; Rhodes and Oreskes 1999; Rhodes et al. 1999; Sillitoe and Burrows 2002). Due to its young age, the massive magnetite of El Laco is the best preserved occurrence of a possible example of an Fe oxide liquid and is thus a critical locality in the debate. On the other hand, if this IOA deposit formed by hydrothermal processes, then the origin of similar deposits will have to be revisited as well.

Recent developments in the analysis and interpretation of trace elements in magnetite demonstrate that it can be used in petrogenetic and provenance studies (Dupuis and Beaudoin 2011; Dare et al. 2012, 2014; Nadoll et al. 2012, 2014; Angerer et al. 2013; Boutroy et al. 2014). In particular, magnetite of hydrothermal origin can be distinguished from that of magmatic origin using a full suite of 25 elements, determined by laser ablation inductively coupled plasma mass spectrometry (LA-ICP-MS), plotted on a multi-element diagram (Fig. 1), based on the partitioning behaviour of elements into magnetite, which facilitates the evaluation of the composition of the fluid/melt that formed the magnetite (Dare et al. 2014). We apply this new technique to magnetite from El Laco, from the massive magnetite samples, from the altered host andesite and from the unaltered host andesite, and argue that the massive magnetite lenses, formerly interpreted as magnetite lava flows, are indeed the product of hydrothermal replacement processes.

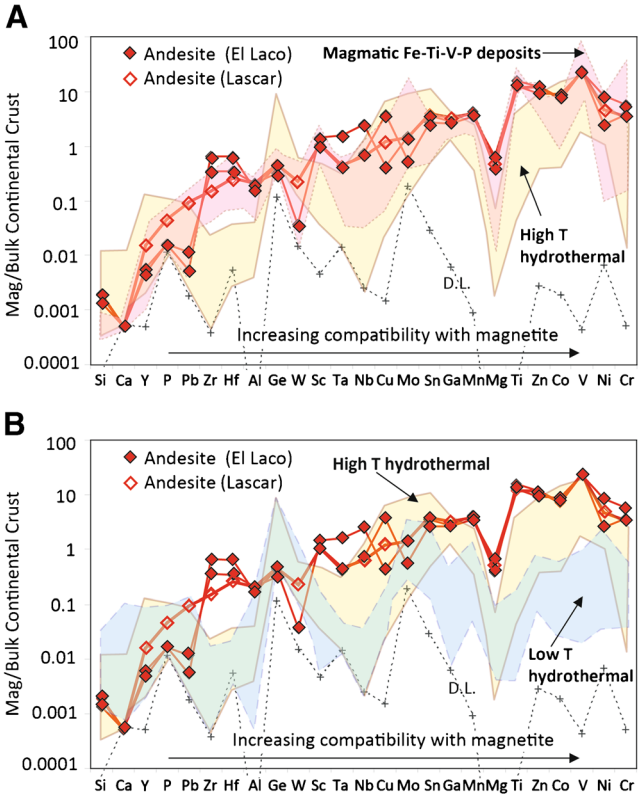

Fig. 1 Multi-element variation diagrams for magnetite from unaltered andesite from El Laco and nearby Lascar volcano (n. Chile) compared to **a** magmatic magnetite from intermediate magmas (Fe-Ti-V and Fe-Ti-P deposits from layered intrusions and anorthosites (*pink field*)) and hydrothermal magnetite from high-temperature (T) deposits (IOCG and porphyry-Cu (*yellow field*)) and **b** hydrothermal magnetite from low-temperature environments (BIF and Fe skarn (*blue fields*)). All data fields are taken from Dare et al. (2014). Normalization to bulk continental crust (values from Rudnick and Gao 2003) and order of elements with increasing compatibility with magnetite to the right. *D.L.* minimum detection limit for a 75-μm beam size

Geology

The calc-alkaline stratovolcano of El Laco in northern Chile comprises andesite and dacite flows and pyroclastic deposits. Detailed descriptions of the geology of El Laco volcano, its massive magnetite "lava flows" and the altered host rocks are given in Nyström and Henríquez (1994), Rhodes et al. (1999), Naslund et al. (2002) and Sillitoe and Burrows (2002). The following is summarized from these works and illustrated with our samples (Fig. 2). The massive magnetite of El Laco consists of 98 % Fe oxide, consisting dominantly of Ti-poor (<0.1 wt%) magnetite with minor hematite and F-rich apatite (<1 %), and trace diopside (<0.01 %). The massive magnetite takes the form of stratabound lenses (e.g. Laco Sur), dikes (e.g. Cristales Grandes) and pyroclastic deposits. The rocks commonly have a slag-like appearance (Fig. 2a), with 20 % open space ("vugs" or "vesicules"). Vertical chimney-like cavities cut across the stratabound magnetite lenses and are lined with euhedral magnetite (Fig. 2b), which is commonly intergrown with blades of diopside or apatite. In the magmatic model, these pipes are interpreted to be fumarolic "gas-escape" tubes through which high-temperature (~800 °C; Broman et al. 1999) gas and aqueous fluids, exsolving from the volatile-rich, Fe oxide liquid, degassed and precipitated euhedral, and in some case zoned, magnetite along the wall linings (Velasco and Tornos 2012).

The footwall of the massive magnetite stratabound lenses comprises jigsaw-puzzle breccia of altered andesite cemented with thin magnetite veins (Sillitoe and Burrows 2002; Fig. 2c). Away from these veins, the amount of magnetite decreases, over a scale of a few millimetres (Fig. 2d), to disseminations and clots of magnetite that clearly replace silicate minerals around their grain boundaries (Fig. 2e). Some of the edges of the magnetite veins are also lined with euhedral magnetite in

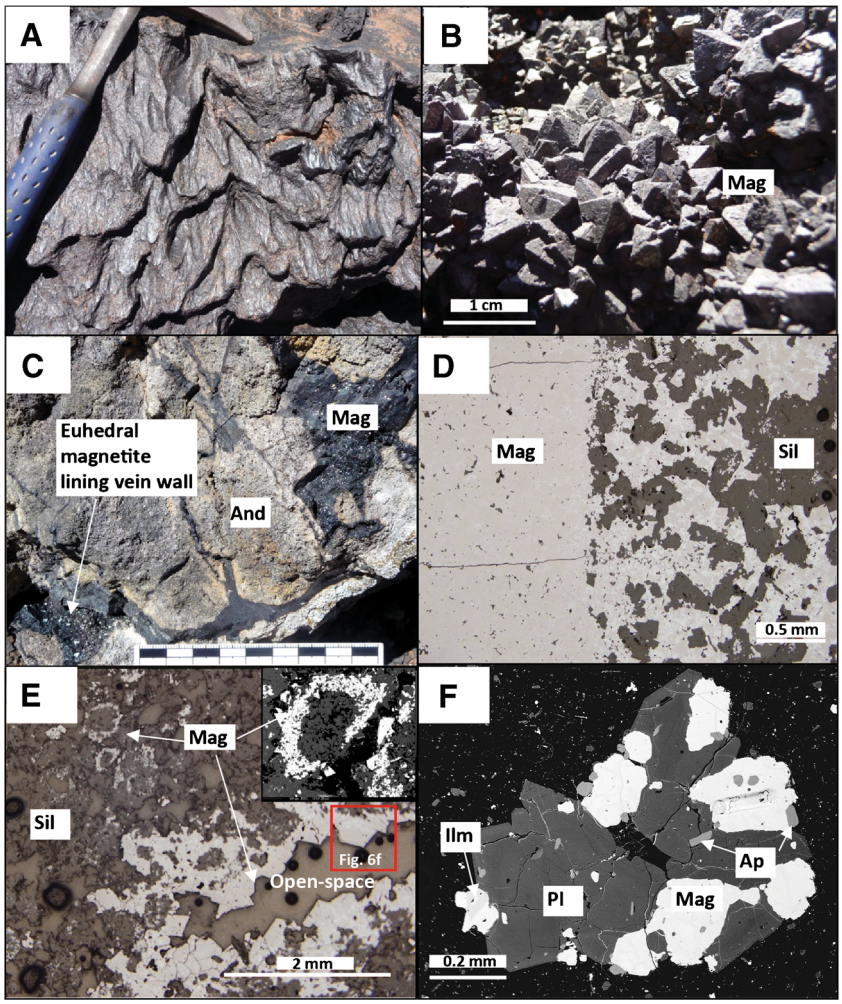

Fig. 2 Textures of massive magnetite "lava flows" (**a**, **b**) and altered andesite host rock (**c**, **d**) from El Laco: **a** "ropey lava surface" of stratabound lens (or wind erosion?); **b** euhedral magnetite (*Mag*) lining "gas-escape pipes"; **c** massive magnetite veins in altered, brecciated andesitic host rock; **d** edge of massive magnetite vein shown in C with a 2–3 mm-wide halo of disseminated magnetite; **e** euhedral magnetite lining open-spaced magnetite vein and rounded clots of magnetite (BSE image (*inset*)) replacing silicate (*Sil*) minerals away from the vein edge (photomicrograph in reflected light); and **f** glomerophenocrysts of magnetite and plagioclase (*Pl*), with minor apatite (*Ap*) and ilmenite (*Ilm*), in a fine-grained matrix in unaltered host andesite of El Laco

vugs (Fig. 2e). In both models, the underlying breccia is interpreted to result from the contact metasomatism of andesite by magnetite-precipitating fluids either (1) from the volatile-rich magmatic fluids that exsolved from the Fe oxide liquid and fractured and altered the host rock (Naslund et al. 2002; Naranjo et al. 2010) or (2) as part of the sequence of hydrothermal alteration that led to the massive replacement of the andesite lava flow (Rhodes et al. 1999; Sillitoe and Burrows 2002).

Sampling and methodology

With a view to establishing whether the magnetite in the massive magnetite of El Laco formed by igneous or hydrothermal replacement processes, we selected samples of magnetite from a number of settings at El Laco (Table 1; Fig. 2). We analysed samples of massive magnetite from the stratabound magnetite lenses, interpreted by some as magnetite lava flows (n=9), mainly from the Laco Sur orebody and from the dike-like orebody of Cristales Grandes (n=1). We compare these with the composition of euhedral magnetite from samples of the supposed gas-escape tubes (n=4) and massive magnetite veins in the altered and brecciated andesite (n=3) both immediately underlying the massive magnetite lens at Laco Sur, as described by Sillitoe and Burrows (2002), and away from any known ore body at Pasos Blancos, as described by Naranjo et al. (2010). All workers agree that these magnetite tubes and veins formed from hydrothermal fluids. Sample descriptions, locations and petrography are given in Supplementary Material. These are then compared with magnetite phenocrysts in unaltered andesite from El Laco volcano itself (Fig. 2f) and nearby Lascar volcano (~100 km northwest of El Laco), which have compositions similar to igneous magnetite (Fig. 1a) and are typical of magnetite from arc-related intermediate magmas (Dare et al. 2014). The unaltered El Laco andesite from this study contains a normal magmatic assemblage comprising phenocrysts of plagioclase (An 70–50), clinopyroxene (Mg# 75), orthopyroxene (Mg# 70–65), hornblende (Fe# 70), magnetite (6 wt% Ti), apatite (2 wt% F) and scarce ilmenite in a fine-grained matrix (Fig. 2f). Results for unaltered andesite are given in Supplementary Material.

Table 1 Sample description, Fe (wt%) and trace element content (ppm) of magnetite (Mag) from El Laco determined by laser ablation (LA)-ICP-MS and electron probe micro-analysis (EPMA), by normal (n) and trace (t) protocols

Geological setting			Magnetite stratabound lens				Magnetite dike		Magnetite vein		Altered host rock				Unaltered host rock[a]	
Location			Laco Sur				Cristales Grandes		Pasos Blancos		Laco Sur				South slope of Laco Peak (and Lascar)	
Description			Massive Mag		Euhedral Mag lining chimney cavities		Massive Mag		Massive Mag		Thin Mag veins in jigsaw breccia		Disseminated Mag in altered andesite		Disseminated Mag in unaltered andesite	
Zoned magnetite			Yes in 6/9 samples		Yes in 2/3 samples		No		No		Yes in both samples		Yes in both samples		No	
Analytical method			LA-ICP-MS	EPMA(n/t)	LA-ICP-MS	EPMA(n/t)	LA-ICP-MS	EPMA(n)	LA-ICP-MS	EPMA(n)	LA-ICP-MS	EPMA(t)	LA-ICP-MS	EPMA(t)	LA-ICP-MS	EPMA(n)
Element and isotope		DL (75 μm)	*N*=8	*N*=9	*N*=3	*N*=4	*N*=1	*N*=1	*N*=1	*N*=1	*N*=2	*N*=2	*N*=2	*N*=2	*N*=3	*N*=3
			n=74	*n*=56	*n*=15	*n*=25	*n*=4	*n*=5	*n*=4	*n*=4	*n*=5	*n*=11	*n*=3	*n*=15	*n*=18	*n*=16
Fe	57	EPMA	70	70	70	70	72	72	73	73	70	70	70	70	60	60
Na	23	0.05	180		n.d.		n.d.		n.d.		n.d.		n.d.		n.d.	
Mg	24	0.01	6,797	7,421	7,694	7,538	5,292	5,036	5,687	5,461	7,473	7,973	6,548	7,087	14,718	13,073
Al	27	0.5	606	595	776	676	984	953	155	142	3,603	4,072	4,986	5,690	15,986	14,077
Si	29	500	4,590	4,693	6,515	4,988	1,897	423	1,617	227	2,724	4,300	35,554	4,063	BDL	490
P	31	5	144		52		28		12		69		70		99	
K	39	2	129	319	n.d.	133	n.d.	n.d.	n.d.	n.d.	n.d.	360	n.d.	513	n.d.	n.d.
Ca	44	4	961	3,428	1,416	1,086	45	n.d.	387	n.d.	680	944	711	964	BDL	23
Sc	45	0.10	0.5		0.6		2.2		0.2		0.3		0.3		26	
Ti	47	0.20	152	BDL	154	BDL	213	BDL	13	BDL	1,046	978	605	738	56,524	60,249
V	51	0.06	1,546	1,853	1,146	BDL	634	BDL	49	BDL	627	BDL	716	BDL	3,291	3,972
Cr	52	0.07	2	BDL	5	BDL	2	BDL	2	BDL	41	BDL	10	BDL	586	803
Mn	55	0.70	416	BDL	330	BDL	889	547	852	720	432	BDL	432	BDL	3,008	2,421
Co	59	0.05	110		117		135		183		123		123		213	
Ni	60	0.40	352	BDL	312	BDL	129	BDL	61	BDL	316	BDL	302	BDL	308	BDL
Cu	63	0.04	11.9	BDL	7.1	BDL	0.3	n.d.	0.3	n.d.	25.9	BDL	39.8	BDL	49	n.d.
Zn	66	0.20	42	BDL	28	BDL	142	BDL	103	BDL	42	BDL	42	BDL	803	817
Ga	71	0.10	6.0		5.0		17.2		0.3		3.8		5.0		50	
Ge	74	0.15	0.43		0.55		0.28		0.17		0.23		0.22		0.53	
Sr	88	0.03	3.2		n.d.		n.d.		n.d.		n.d.		n.d.		n.d.	
Y	89	0.01	4.05		3.74		0.02		0.60		1.69		0.82		0.17	
Zr	90	0.02	1.04		1.02		0.92		0.21		3.66		1.89		55	
Nb	93	0.02	9.91		5.01		0.56		1.88		2.01		1.13		10.20	
Mo	95	0.15	0.72		0.20		0.31		0.25		1.24		1.00		0.92	
Sn	118	0.05	16.90	BDL	8.12	BDL	5.40	n.d.	9.95	n.d.	6.75	BDL	6.46	BDL	5.74	n.d.
Ba	137	0.01	3.3		n.d.		n.d.		n.d.		n.d.		n.d.		n.d.	
La	139	0.01	9.61		3.86		0.03		1.95		4.22		3.94		0.13	
Sm	147	0.05	1.33		0.93		0.07		0.13		0.50		0.54		0.06	
Yb	172	0.02	0.65		0.53		0.02		0.15		0.22		0.06		0.04	
Hf	178	0.02	0.01		0.01		0.01		0.01		0.19		0.13		1.53	

Table 1 (continued)

Geological setting			Magnetite stratabound lens			Magnetite dike	Magnetite vein	Altered host rock			Unaltered host rock[a]
Ta	181	0.01	0.24		0.43	0.07	0.02	0.15		0.12	0.57
W	182	0.02	0.67		0.07	0.02	0.01	0.23		0.03	0.09
Pb	208	0.02	0.44		0.12	0.15	0.19	0.35		0.24	0.41
Ni/Cr			176		65	62	33	8		30	0.60

DL detection limit of LA-ICP-MS in ppm, *N* number of samples, *n* number of analyses, *n.d.* not determined, *BDL* below detection limit (values given in main text)

[a] LA-ICP-MS data of magnetite from unaltered host rock taken from Dare et al. (2014) with additional REE data from this study

The content of 25 trace elements (Mg, Al, Si, P, Ca, Sc, Ti, V, Cr, Mn, Co, Ni, Cu, Zn, Ga, Ge, Y, Zr, Nb, Mo, Sn, Hf, Ta, W and Pb) was determined in magnetite by LA-ICP-MS at LabMaTer, UQAC (Table 1) following the analytical protocol of Dare et al. (2014), with the addition of some elements not commonly reported in magnetite (Na, K, rare earth elements (REE), Ba and Sr) for some samples. The LA-ICP-MS system at UQAC comprises a Resonetics M-50 193 nm laser coupled with an Agilent 7700x ICP-MS. The international reference material (GSE-1 g) was used for calibration, and ^{57}Fe was used as the internal standard. A beam size of 55–75 μm was used to ablate lines across magnetite grains to observe any zonation. Iron and minor elements were also determined by electron probe micro-analysis (EPMA) at Université Laval (Quebec, Canada) following normal and trace protocols described in Dare et al. (2012). Detection limits (in ppm) for the normal protocol of EPMA are Mg, 150; Al, 140; Si, 130; Ti, 360; V, 1,690; Cr, 570; Mn, 320; Ni, 420; and Zn, 600. Detection limits (in ppm) for the trace protocol are Mg, Al, Si and Ti, 20 each; V and Cr, 50 each; Mn, 40; Ni, 60; Zn, 100; Cu, 80; K, 10; Sn, 50; and Ca, 20. Zoning in magnetite was mapped using (1) EPMA at Université Laval for Si, Ca, Mg and Al and (2) LA-ICP-MS with a 15–19-μm beam size for a number of trace elements (Dare et al. 2014). Complete results are given in Supplementary Material. Average compositions for each rock type are presented in Table 1.

Magnetite from the massive samples and altered host rock of El Laco are compared to magnetite from known magmatic and hydrothermal environments using multi-element diagrams (Figs. 1 and 3), which allow a direct comparison of the chemical signature of magnetite, for a full suite of trace elements, from different settings (e.g. Dare et al. 2014).

Results

Magnetite chemistry

The trace element patterns of magnetite from El Laco massive magnetite are plotted on the multi-element diagram in Fig. 3a. Our samples of massive magnetite are representative of the magnetite lava flows at El Laco as they have the same compositional range, for the ten elements previously published by Nyström and Henríquez (1994), as magnetite concentrates from all the deposits of El Laco (Fig. 3a). Although there is some natural variation among samples, up to one order of magnitude for some elements (e.g. Ti, Mo, Nb, Ca and Si), all the massive samples have the same general pattern. The composition of the massive magnetite lenses is similar to magnetite forming veins and disseminations replacing silicate minerals (Fig. 2c–e) in the altered, brecciated host rock (hereafter termed breccia-hosted magnetite) although the breccia-hosted magnetite is slightly richer in Ti, Al, Zr and Hf

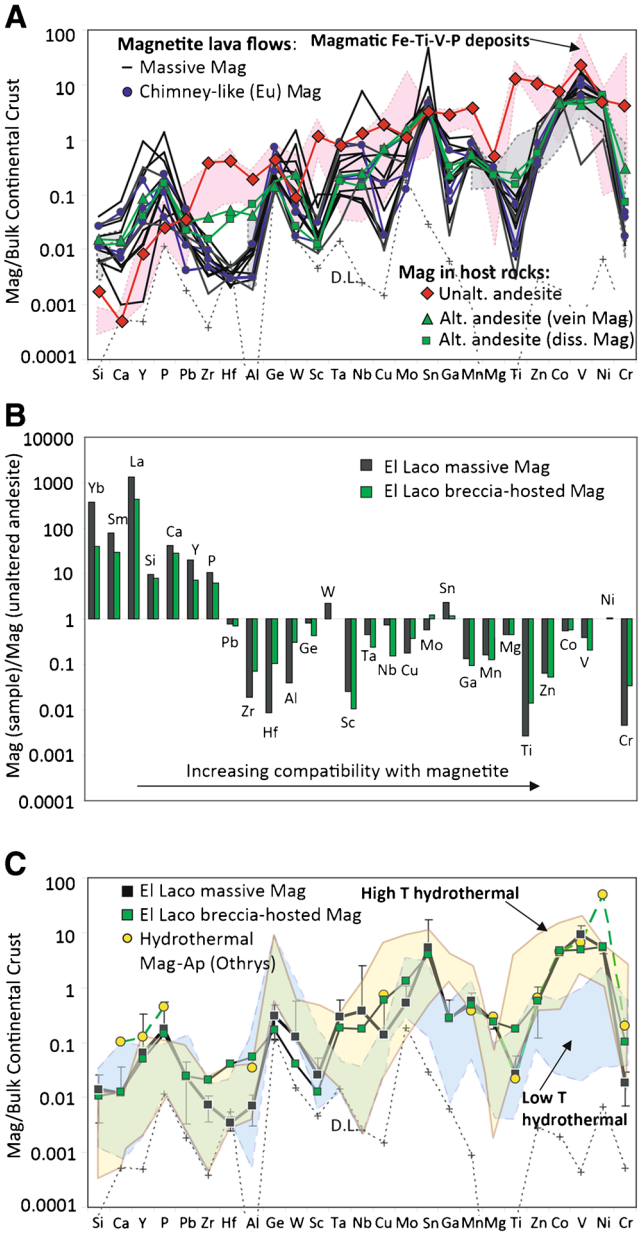

Fig. 3 Composition of magnetite (*Mag*) from El Laco: **a** magnetite from massive magnetite deposits compared to magnetite in host andesite (both unaltered and altered). Compositional range of magnetite data from El Laco massive magnetite deposits (*grey field*; Nyström and Henríquez 1994) and magmatic Fe-Ti-V-P deposits (*pink field*; Dare et al. 2014) for comparison. **b**, **c** Magnetite from El Laco massive magnetite deposits compared to that in altered (alt.), brecciated andesitic host rocks (both disseminated and vein magnetite). In **c**, compositional range of magnetite from high-temperature (*yellow field*) and low-temperature (*blue field*) hydrothermal environments is shown (fields from Dare et al. 2014). Magnetite data for hydrothermal magnetite-apatite (Ap) deposited in shear zone of Othrys ophiolite from Mitsis and Economou-Eliopoulos (2001). Normalization of magnetite data by bulk continental crust (values from Rudnick and Gao 2003) in **a** and **c** and by the average composition of primary magnetite in unaltered andesite of El Laco in **b**. Order of elements is with increasing compatibility with magnetite from left to right. *D.L.* detection limit for 75-μm beam size

(Fig. 3a, b). Both massive magnetite and breccia-hosted magnetite are different to any known magmatic magnetite including that in unaltered andesite at El Laco (Fig. 3a, b) and are similar in composition to that of high-temperature hydrothermal magnetite (Fig. 3c), as shown below:

1. Magnetite from El Laco massive magnetite samples and brecciated, altered andesite is strongly depleted in Ti, Al, Cr, Zr, Hf and Sc relative to magmatic magnetite in unaltered andesite (Fig. 3b). These elements are considered relatively immobile in hydrothermal fluids and are characteristically low in magnetite formed in hydrothermal environments (Fig. 1; Dare et al. 2014). The high Ni/Cr ratio (>1) of El Laco massive magnetite and breccia-hosted magnetite is also typical of hydrothermal magnetite and distinguishes it from all magmatic magnetite (Fig. 4), including Ti-poor magnetite from felsic melts (Dare et al. 2014). This is because the behaviour of Ni and Cr is decoupled in fluids due to differences in solubility/mobility, whereas they behave the same way in magmatic systems as they are both compatible during fractionation of the silicate melt (Dare et al. 2014).
2. Magnetite from El Laco massive magnetite and brecciated, altered andesite is enriched in elements that are highly incompatible into magnetite in magmatic systems, such as Si, Ca, Na, Y, P and even REE, and normally in very low abundance in magmatic magnetite (Figs. 3b and 5) but can be enriched in hydrothermal magnetite (Fig. 1). The REE and Y normalized patterns for in situ analyses of

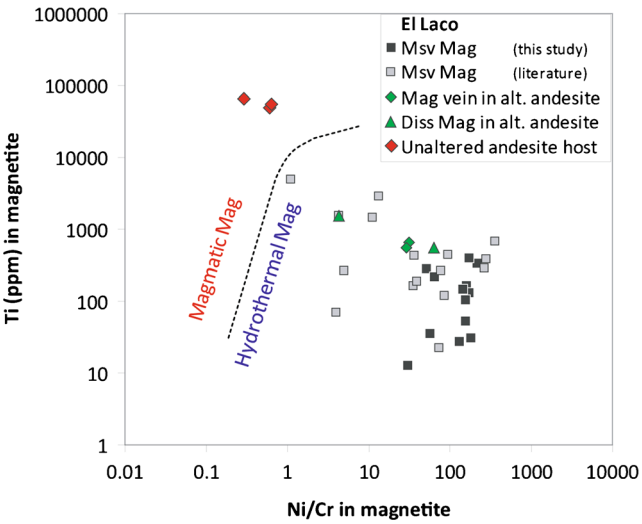

Fig. 4 Plot of Ti (ppm) versus Ni/Cr ratio (un-normalized) in magnetite (Mag) to discriminate magnetite from magmatic and hydrothermal environments (after Dare et al. 2014). Magnetite from El Laco massive (msv) magnetite and altered (alt.), brecciated host andesite plot in hydrothermal field whereas magnetite from unaltered andesite plots in magmatic field. All data sources for magmatic and hydrothermal settings are taken from the compilation in Dare et al. (2014). Literature data for El Laco massive magnetite is from Nyström and Henríquez (1994)

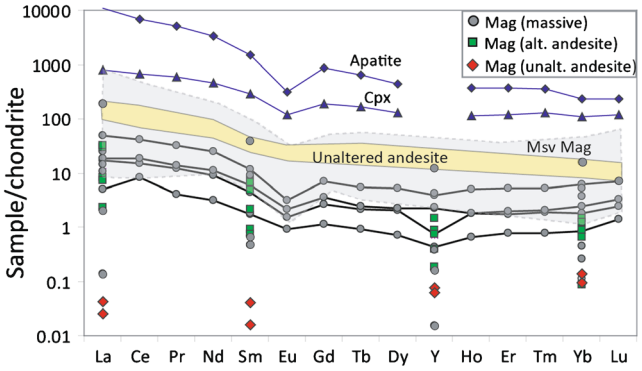

Fig. 5 REE distribution patterns, normalized to chondrite values (Lodders 2003), of magnetite (Mag) from El Laco analysed by LA-ICP-MS (this study) from massive magnetite (*grey circle*), altered (*alt.*) andesite (*green square*) and unaltered (*unalt.*) andesite (*red diamond*). Data of El Laco from Rhodes et al. (1999) for massive magnetite (whole rock: *grey field*), unaltered andesite (whole rock: *yellow field*), and apatite and clinopyroxene (*Cpx*) mineral separates are plotted for comparison

magnetite from this study are similar, showing slight enrichment in the light REE, between magnetite in the massive magnetite samples, including euhedral magnetite in "gas-escape tubes", and magnetite in veins in the altered host rock (Fig. 5). In contrast, the REE contents in magnetite from unaltered andesite lava at El Laco are close to or less than detection (Fig. 5). The LA-ICP-MS data of magnetite is very similar to whole-rock data of magnetite samples analysed by Rhodes et al. (1999) from a variety of deposits at El Laco (Fig. 5). El Laco massive magnetite is similar to the whole-rock pattern of unaltered andesite, except for a negative Eu anomaly and typically lower total abundance of REE in the massive magnetite. Minor amount of apatite and clinopyroxene in the El Laco ore contains a higher abundance, but a similar pattern, of REE compared to magnetite (Fig. 5). The presence of REE in magnetite has also been reported from other IOA (Kiruna-type) deposits in addition to magnetite from some banded iron formations (Frietsch and Perdahl 1995).

3. The trace element-normalized pattern of magnetite from the massive magnetite and the altered, brecciated host rocks at El Laco (Fig. 3c) is most similar to that of hydrothermal magnetite from high-temperature environments (>500 °C) and different to the pattern of magnetite in low-temperature (<500 °C) environments, which have typically lower in Ni, V, Co, Zn and Sn contents (Fig. 1; Dare et al. 2014). One exception, however, is the low-temperature (~300 °C) deposition of magnetite, together with apatite, in a shear zone of the Othrys ophiolite (Mitsis and Economou-Eliopoulos 2001). In this case, the high Mg, Ni, Co and Zn contents probably reflect the mafic/ultramafic source rocks (Dare et al. 2014). Although its chemical pattern is similar to that of El Laco (Fig. 3c), the host rocks at El Laco are intermediate in composition, and thus the relatively high content of Ni, V, Co, Zn and Sn in magnetite at El Laco more likely results from precipitation from high-temperature fluids rather than from lower-temperature fluids with a mafic/ultramafic source.

Oscillatory zoning in magnetite

Zoning is visible, both in reflected light- and back-scattered imaging, in euhedral magnetite that line the walls of the supposed gas-escape tubes (Fig. 6a), as previously reported by Velasco and Tornos (2012). We found that magnetite in half of the massive magnetite samples, both fine and coarser grained varieties, also displays oscillatory zoning (both euhedral and more rounded in shape: Fig. 6b–e) including samples that could be interpreted to have a ropey lava texture (Fig. 2a). The zonation can be complex with truncations and resorption features (Fig. 6b–d). Euhedral magnetite lining veins in the underlying brecciated andesite (Fig. 2e) also displays oscillatory zoning (Fig. 6f) identical in form and chemistry to magnetite in the gas-escape tubes and in the massive magnetite samples. In all three cases, the oscillatory zoning of magnetite is characterized by micrometre-scale layers enriched in Si (<1.5 wt%, Fig. 6d), Ca (<0.25 wt%), Mg (<1 wt%), Na (<200 ppm) and REE (<50 ppm total REE) alternating with layers depleted in these elements. LA-ICP-MS mapping of the zoned magnetite (Fig. 7) shows that the Si-rich layers are also relatively enriched in elements considered not only immobile, e.g. Al and high field strength elements (HFSE: P, Sc, Ti, V, Y, Zr, Nb and Ta), but also enriched in the large ion lithophile elements (LIL: K, Sr, Ba), which are mobile in hydrothermal fluids. Other elements, such as Cr, Ni, Co, Zn and Sn, however, show no obvious change in abundance. This oscillatory zoning is strikingly similar to that present in Si-rich magnetite from the Fe skarn of Vegas Peledas, although the overall composition is different (Dare et al. 2014). Such zoning in Fe skarn is indisputably hydrothermal in origin and attributed to magnetite growth during fluctuating conditions/composition of the fluid (e.g. Shimazaki 1998).

Discussion

New in situ trace element analysis and petrographic observations of magnetite from the El Laco massive magnetite lenses and encasing volcanic rocks provide new constraints on the two opposing models of formation of the supposed magnetite lava flows, as discussed below. The similarity of the trace element signature, including oscillatory zoning and REE content, of magnetite in massive magnetite lava flows with that of magnetite replacing the altered, brecciated andesite host rocks suggests a common origin. Magnetite from both the massive

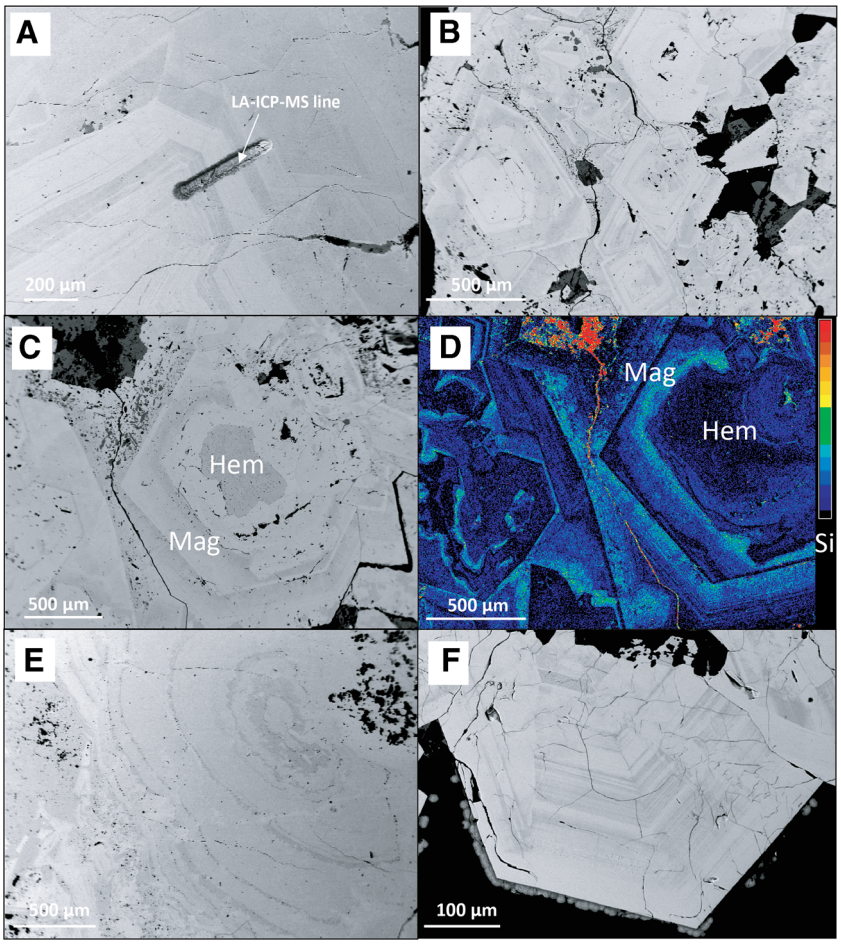

Fig. 6 Oscillatory zoning in magnetite (Mag) from El Laco: **a** euhedral magnetite lining "gas escape pipe" (sample LC13). **b–d** Massive magnetite with "ropey surface" texture (ELC7 shown in Fig. 2a). In **c–d**, magnetite replacing hematite (*Hem*), preserved in centre, and complex zonation pattern with truncations, overgrowths and resorption features. **e** Zonation pattern highlights rounded growth of magnetite (LC9). **f** Euhedral magnetite lining the open-space vein in the altered, brecciated andesite host rock (ELC1 show in Fig. 2d) displaying similar oscillatory zoning. All images are from back-scattered electrons except **d** which is an electron microprobe X-ray map of Si, where high Si is represented by *light blue colour*

magnetite samples and brecciated, altered andesite is very different in composition to magnetite from unaltered andesite, and all known magmatic Fe oxide deposits, but is more similar in composition to magnetite formed from high-temperature (>500 °C) hydrothermal fluids with a magmatic source, such as IOCG and porphyry-Cu deposits (Figs. 1 and 3). Consequently, our preferred interpretation is that the El Laco Fe oxide deposits formed by high-temperature hydrothermal replacement processes.

Constraints on hydrothermal replacement model

The origin of oscillatory-zoned, Si-rich magnetite rimming open-spaced structures, such as along the "gas-escape tubes" in the massive stratabound lenses (Figs. 2b and 6a) and in parts of the magnetite veins in the underlying altered host rock (Figs. 2d and 6f), is relatively easy to reconcile with fluctuating physio-chemical parameters and composition of the fluid during magnetite growth in the hydrothermal model (e.g. Sillitoe and Burrows 2002) or gas in the case of the magmatic model (e.g. Velasco and Tornos 2012). However, the occurrence of identical oscillatory zoning of Si-rich magnetite in half of the samples of massive magnetite implies that a similar process, similar to that in forming zoned Si-rich magnetite in Fe skarns (Shimazaki 1998; Dare et al. 2014), was also important in forming part of the massive magnetite, interpreted by some as lava flows. This strongly favours the complete replacement of the pre-existing andesite by dissolution and precipitation of magnetite by hydrothermal open-space filling, as argued by Rhodes et al. (1999) and Sillitoe and Burrows (2002). Based on the similarity of the REE normalized patterns of massive magnetite and unaltered whole-rock andesite (Fig. 5), Rhodes et al. (1999) suggested that the REE in magnetite were inherited from the protolith during alteration. The zoned distribution of the immobile elements (HFSE including the REE, Fig. 7b–c) in magnetite suggests that at least a part of these elements were released during the dissolution of silicates but were only locally remobilized (perhaps on the grain scale) and were incorporated, with silica, into magnetite episodically during its precipitation from the fluids. The truncations of the layering in magnetite (Fig. 6b–d) indicate that magnetite itself underwent episodic dissolution and re-precipitation from the fluids (c.f. Hu et al. 2014).

We agree with Sillitoe and Burrows (2002) that replacement was focused originally around fractures, allowing the fluids to permeate a selectively porous horizon in the host-rock and gradually replace the silicate minerals, starting at

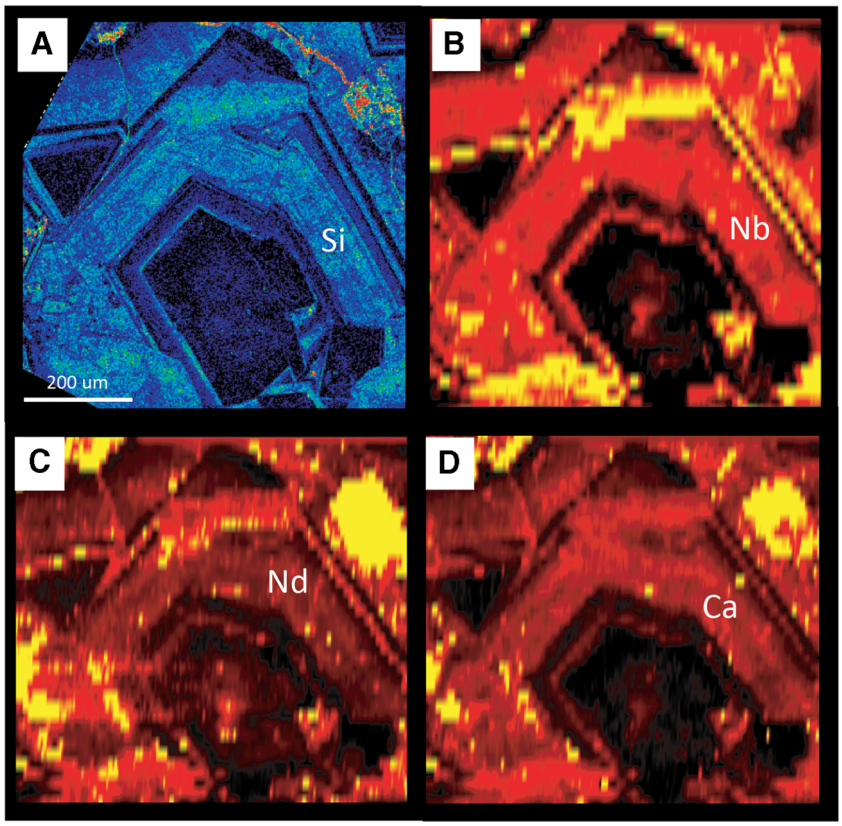

Fig. 7 Chemical maps of oscillatory zoned magnetite from El Laco massive magnetite (sample ELC7 shown in Figs. 2a and 6b). **a** Electron microprobe X-ray map of Si (beam size 3 μm). High Si represented by *light blue colour*. **b**–**d** Nb, Nd and Ca mapped by laser ablation ICP-MS (beam size 19 μm). Highest contents of these elements are represented by *yellow colour*

grain boundaries by magnetite near the edge of the veins (Fig. 2e). This process continued with an increase in fluid-rock interaction until all the silicate material was replaced mainly by magnetite. In other words, the process that formed the massive veins on a centimetre scale in the brecciated andesite shown in Fig. 2c could be extrapolated to the metre scale to form the massive magnetite lenses itself. According to Sillitoe and Burrows (2002) the dissolution-precipitation process will create porosity and crystal-lined vugs/chimneys (e.g. Fig. 2b, c) in the same way that hollow chimneys, enclosed by chalcedony, form in shallow-level, epithermal veins. We propose that the open-spaced fractures that allowed the passage of the fluids during the replacement of andesite at El Laco are in part recorded by oscillatory-zoned magnetite in both the massive magnetite lenses and in the brecciated footwall. Selective replacement by magnetite along specific permeable horizons and preservation of primary textures is common in IOCG settings (Corriveau et al. 2010). However, some of the ropey lava-like textures preserved in the massive magnetite lenses could simply represent fierce wind erosion (Fig. 2a), which is known to sculpt volcanic rocks in a similar way in the Andes (J. Richardson pers. comm.).

Previous work suggested that although the early, widespread sodic (−potassic) and calcic (diopside) alteration of the host andesite (Rhodes et al. 1999) formed from extremely hot (710–840 °C) and hypersaline fluids (Sheets et al. 1997; Broman et al. 1999; Rhodes et al. 1999), the magnetite deposition occurred at relatively low temperatures based on fluid inclusions in apatite (250–350 °C; Sheets et al. 1997) hosted in the massive magnetite. However, Rhodes and Oreskes (1999) suggested that the hydrothermal fluids that formed the magnetite deposits had a magmatic contribution, in order to explain the F-rich rather than Cl-rich composition of the apatite. They proposed that the fluids resulted from the interaction of the andesite magma body with buried evaporate deposits. Evaporate deposits are common in the arid setting of the Andes and have been suggested to be an important ligand source for forming igneous-related Fe oxide-(REE-Cu-Au-U) mineralization (Barton and Johnson 1996). The new trace element data for magnetite from the El Laco massive magnetite deposits indicate that the fluids involved were hot (>500 °C) with a magmatic contribution, based on the similarity of the magnetite normalized patterns with those from porphyry-Cu and IOCG deposits (Fig. 3). This is consistent with the high-temperature (850–450 °C) estimates of magnetite (see review in Naslund et al. 2002) based on magnetite remnant magnetism and pyroxene compositions in massive magnetite, including the gas-escape tubes. Therefore, we concur with Sillitoe and Burrows (2003) that the precipitation of magnetite from fluids was relatively early at high temperatures, whereas apatite precipitated only locally as the fluids cooled to lower temperatures, around 250–350 °C (Sheets et al. 1997).

Constraints on magmatic model

Our geochemical results and petrographic observations of magnetite from El Laco massive magnetite deposits, and altered host rocks, place important constraints on any future experimental work which aims to saturate andesite magma with an immiscible Fe oxide liquid. The experiments must be able to not only reproduce the unusual trace element composition of El Laco magnetite but also explain the oscillatory zonation of magnetite during rapid eruption of such an Fe oxide liquid. Our in situ trace element data of magnetite from the gas-escape tubes and veins in the brecciated footwall rocks places further constraints on the magmatic model, whereby it is proposed that magnetite in these environments formed from a fluid/gas phase that exsolved from the volatile-rich Fe oxide liquid (Naslund et al. 2002; Naranjo et al. 2010; Velasco and Tornos 2012). We have shown that magnetite from the massive lenses, which in the magmatic model crystallized from the Fe oxide liquid, is identical in composition, and zoning, to magnetite from the gas-escape tubes and veins in the footwall. In the magmatic model, this would mean that magnetite crystallizing from the Fe oxide liquid has exactly the same composition as magnetite precipitating from an exsolved fluid/gas phase (Naslund pers. comm.) and that there is no partitioning of trace elements between the Fe oxide liquid and Fe-rich fluid/gas phase. This will need to be demonstrated in future experiments.

Experiments have shown that it is possible to saturate an intermediate magma (ferrodiorite) in an immiscible Fe-rich liquid by the addition of a large amount of P (>10 wt% P_2O_5), but the Fe-rich liquid is not pure and contains a moderate amount (5–20 wt%) of SiO_2, among other elements including Ca, P, Mg, Al and Ti (Tollari et al. 2008). In this case, a normal magmatic assemblage of Fe-Ti oxides (Ti-rich magnetite±ilmenite) crystallizes together with apatite and silicate minerals (Tollari et al. 2008) and represents a possible analogue for forming Fe-Ti-P deposits associated with ferrogabbro/norites in layered intrusions and anorthosite complexes (e.g. Chen et al. 2013; Zhou et al. 2013). More recent experiments by Lester et al. (2013) showed that it is also possible to form an Fe-P-rich immiscible melt, containing 10–40 wt% SiO_2, with the addition of a lower amount of P (5 wt% P_2O_5) in the presence of volatiles (10 wt% H_2O and 1–2 wt% of S, F or Cl). Such volatile and P-rich conditions are thought to be important in forming the proposed Fe oxide liquid at El Laco (Tornos et al. 2011; Naslund pers. comm.). However, Lester et al. (2013) showed that even under these volatile-rich conditions, all the transition elements (including Ni, Cr, V) and HFSE (including Ti and REE) partitioned preferentially into the Fe-rich melt over the Si-rich melt. In summary, any Fe-rich liquid that was in equilibrium with, and segregated from, silicate magma of intermediate composition should crystallize Fe-Ti-oxides and not pure magnetite (i.e. Ti-Al poor), which is characteristic of El Laco and other Kiruna-type magnetite deposits.

The large amount of P (5–10 wt% P_2O_5) required to saturate a magma in an Fe-rich liquid cannot be reached by simple fractional crystallization alone because saturation of the magma in apatite or a phosphate phase would occur first, at a much lower P content (0.5–2 wt% P_2O_5; Harrison and Watson 1984; Toplis et al. 1994; Tollari et al. 2008), before the magma saturated in an immiscible Fe-rich liquid. However, it may be possible to trigger Fe-rich liquid immiscibility by magma-mixing (Clark and Kontak 2004) or by assimilation of P-rich country rock, such as evaporate deposits/salars which common near El Laco volcano. But, what special chemical ingredient and/or condition/s is needed to produce a pure Fe oxide liquid (with<1 wt% Si), low in Ti, Al and other HFSE, which was not in chemical equilibrium with the intermediate magma of El Laco volcano? Pure Fe oxide liquid has been made by simply mixing Fe, C and O in the high-temperature (800–900 °C) experiments of Weidner (1982), but can it be formed from an andesitic starting composition and what would the partitioning behaviour of trace elements be between such an Fe oxide liquid and its parental andesitic magma? Until a pure Fe oxide liquid and its exsolving gas phase, which can reproduce the chemistry of El Laco magnetite from both the massive lenses and the veins in the brecciated footwall rocks, are produced in the laboratory, the simplest explanation for the El Laco magnetite deposits is that of hydrothermal replacement of andesite lava flows by high-temperature magmatic-hydrothermal fluids.

Conclusions

We have applied a new analytical technique to place new constraints on the on-going debate over the origin of the enigmatic massive magnetite deposits of El Laco, northern Chile. In situ analyses and geochemical mapping of magnetite, by laser ablation ICP-MS and electron probe micro-analysis, of samples from the massive magnetite stratabound lenses, interpreted by some as magnetite lava flows, are compared to those from both altered and unaltered host rock andesite. Magnetite from massive magnetite is most similar in composition and displays the same oscillatory zoning, as magnetite in the brecciated, altered host rock. Both massive and breccia-hosted magnetite are dissimilar to magmatic magnetite in the unaltered andesite and all other magmatic magnetite. The trace element normalized pattern of magnetite from the massive ores and altered host rock is most similar to magnetite from high-temperature hydrothermal deposits, such as porphyry-Cu and Fe oxide-copper-gold deposits. This new data agrees best with the hydrothermal model for the complete replacement of pre-existing andesite lava flows by the dissolution of the silicate minerals and precipitation of magnetite. Oscillatory zoning of magnetite records fluctuating fluid composition and/or physio-chemical conditions during magnetite growth.

Acknowledgments This project was funded by NSERC, DIVEX, Vale, the Canadian Research Chair in Magmatic Metallogeny, and in part by the Geological Survey of Canada's TGI4 program. We thank S. Medhi, D. Savard and M. Choquette for their assistance with laser ablation-ICP-MS and microprobe analyses, respectively. We thank SGA Chilean guides and D. Genna for their aid with sample collection and photos. Thanks are given to F. Tornos and L. Fontboté for additional samples from El Laco and to H. Mumin, L. Corriveau, J. Richards and D. Naslund for interesting and stimulating discussions. We are very grateful to comments from 3 reviewers (D. Burrows, D. Naslund and 1 anonymous) and Editor, B. Lehmann.

References

Angerer T, Hagemann SG, Danyushevsky L (2013) High-grade iron ore at Windarling, Yilgarn Craton: a product of syn-orogenic deformation, hypogene hydrothermal alteration and supergene modification in an Archean BIF-basalt lithostratigraphy. Mineral Deposita 48:697–728

Barton MD, Johnson DA (1996) Evaporitic-source model for igneous-related Fe oxide–(REE-Cu-Au-U) mineralization. Geology 24:259–262

Boutroy E, Dare SAS, Beaudoin G, Barnes S-J, Lightfoot PC (2014) Magnetite composition in Ni-Cu-PGE deposits worldwide and its application to mineral exploration. J Geochem Explor 145:64–81

Broman C, Nyström JO, Henríquez F, Elfman M (1999) Fluid inclusions in magnetite-apatite ore from a cooling magmatic system at El Laco, Chile. GFF 121:253–267

Chen WT, Zhou M-F, Zhao T-P (2013) Differentiation of nelsonitic magmas in the formation of the ~1.74 Ga Damiao Fe–Ti–P ore deposit, North China. Contrib Mineral Petrol 165:1341–1362

Clark AH, Kontak DJ (2004) Fe-Ti-P oxide melts generated through magma mixing in the Antauta subvolcanic center, Peru: implications for the origin of nelsonite and iron oxide-dominated hydrothermal deposits. Econ Geol 99:377–395

Corriveau L, Williams PJ, Mumin AH (2010) Alteration vectors to IOCG mineralization from uncharted terrains to deposits. In: Corriveau L, Mumin AH (eds) Exploring for iron oxide copper gold deposits: Canada and global analogues. The Geological Association of Canada, St. John's, pp 89–110

Dare SAS, Barnes S-J, Beaudoin G (2012) Variation in trace element content of magnetite crystallized from a fractionating sulfide liquid, Sudbury, Canada: implications for provenance discrimination. Geochim Cosmochim Acta 88:27–50

Dare SAS, Barnes S-J, Beaudoin G, Méric J, Boutroy E, Potvin-Doucet C (2014) Trace elements in magnetite as petrogenetic indicators. Miner Depos 49:785-796

Dupuis C, Beaudoin G (2011) Discriminant diagrams for iron oxide trace element fingerprinting of mineral deposit types. Mineral Deposita 46:319–335

Frietsch R, Perdahl J-A (1995) Rare earth elements in apatite and magnetite in Kiruna-type iron ores and some other iron ore types. Ore Geol Rev 9:489–510

Harrison TM, Watson EB (1984) The behavior of apatite during crustal anatexis: equilibrium and kinetic considerations. Geochim Cosmochim Acta 48:1467–1477

Hildebrand RS (1986) Kiruna-type deposits; their origin and relationship to intermediate subvolcanic plutons in the Great Bear magmatic zone, Northwest Canada. Econ Geol 81:640–659

Hu H, Li J-W, Lentz D, Ren Z, Zhao X-F, Deng X-D, Hall D (2014) Dissolution–reprecipitation process of magnetite from the Chengchao iron deposit: insights into ore genesis and implication for in-situ chemical analysis of magnetite. Ore Geol Rev 57:393–405

Jonsson E, Troll VR, Högdahl K, Harris C, Weis F, Nilsson KP, Skelton A (2013) Magmatic origin of giant 'Kiruna-type' apatite-iron-oxide ores in Central Sweden. Scientific reports 3

Lester G, Clark A, Kyser T, Naslund H (2013) Experiments on liquid immiscibility in silicate melts with H_2O, P, S, F and Cl: implications for natural magmas. Contrib Mineral Petrol 166:329–349

Lodders K (2003) Solar system abundances and condensation temperatures of the elements. Astrophys J 591:1220

Mitsis I, Economou-Eliopoulos M (2001) Occurrence of apatite associated with magnetite in an ophiolite complex (Othrys), Greece. Am Mineral 86:1143–1150

Nadoll P, Mauk JL, Hayes TS, Koenig AE, Box SE (2012) Geochemistry of magnetite from hydrothermal ore deposits and host rocks of the Mesoproterozoic Belt Supergroup, United States. Econ Geol 107: 1275–1292

Nadoll P, Angerer T, Mauk JL, French D, Walshe J (2014) The chemistry of hydrothermal magnetite: a review. Ore Geol Rev 61:1–32

Naranjo JA, Henríquez F, Nyström JO (2010) Subvolcanic contact metasomatism at El Laco Volcanic Complex, Central Andes. Andean Geol 37:110–120

Naslund H, Henríquez F, Nyström J, Vivallo W, Dobbs F (2002) Magmatic iron ores and associated mineralization: examples from the Chilean High Andes and Coastal Cordillera. Hydrothermal Iron Oxide Copper-Gold Relat Depos: Glob Perspect 2:207–226

Nyström J, Henríquez F (1994) Magmatic features of iron ores of the Kiruna type in Chile and Sweden: ore textures and magnetite geochemistry. Econ Geol 89:820–839

Park CF (1961) A magnetite "flow" in northern Chile. Econ Geol 56: 431–441

Rhodes A, Oreskes N (1999) Oxygen isotope composition of magnetite deposits at El Laco, Chile: evidence of formation from isotopically heavy fluids. Soc Econ Geol Spec Publ 7:333–351

Rhodes AL, Oreskes N, Sheets S (1999) Geology and rare earth element geochemistry of magnetite deposits at El Laco, Chile. Soc Econ Geol Spec Publ 7:299–332

Rudnick R, Gao S (2003) Composition of the continental crust. Treatise Geochem 3:1–64

Sheets S, Oreskes N, Rhodes A, Bodnar R, Szabo C (1997) Fluid inclusion evidence for a hydrothermal origin for magnetite-apatite mineralization at El Laco, Chile. Geological Society of America, Abstracts with Programs. pp A50

Shimazaki H (1998) On the occurrence of silician magnetites. Resour Geol 48:23–29

Sillitoe RH, Burrows DR (2002) New field evidence bearing on the origin of the El Laco magnetite deposit, northern Chile. Econ Geol 97: 1101–1109

Sillitoe RH, Burrows DR (2003) New field evidence bearing on the origin of the El Laco magnetite deposit, northern Chile—a reply. Econ Geol 98:1501–1502

Tollari N, Baker D, Barnes S-J (2008) Experimental effects of pressure and fluorine on apatite saturation in mafic magmas, with reference to layered intrusions and massif anorthosites. Contrib Mineral Petrol 156:161–175

Toplis MJ, Libourel G, Carroll MR (1994) The role of phosphorus in crystallisation processes of basalt: an experimental study. Geochim Cosmochim Acta 58:797–810

Tornos F, Velasco F, Morata D, Barra F, Rojo M (2011) The magmatic-hydrothermal evolution of the El Laco as tracked by melt inclusions and isotope data In: Barra F, Reich M, F T (eds) Proceedings of the 11th Biennial SGA Meeting. Antofagasta, Chile, pp 443–445.

Velasco F, Tornos F (2012) Insights on the effects of hydrothermal alteration in the El Laco magnetite deposit. Macla 16:210–211

Weidner JR (1982) Iron-oxide magmas in the system Fe-C-O. Can Mineral 20:555–566

Zhou M-F, Chen WT, Wang CY, Prevec SA, Liu PP, Howarth GH (2013) Two stages of immiscible liquid separation in the formation of Panzhihua-type Fe-Ti-V oxide deposits, SW China. Geosci Front 4:481–502